Inverse Monte-Carlo and Demon Methods for Effective Polyakov Loop Models of $SU(N)$-YM

T. Heinzl[a], T. Kästner[b], S. Uhlmann[b], B. H. Wellegehausen[b], A. Wipf[b], C. Wozar[b]

[a]School of Mathematics and Statistics, University of Plymouth, Drake Circus, Plymouth, PL4 8AA, United Kingdom

[b]Theoretisch-Physikalisches Institut, Friedrich-Schiller-Universität Jena, Max-Wien-Platz 1, 07743 Jena, Germany

Introduction

The Svetitsky-Yaffe conjecture states that the Yang-Mills finite temperature transition in dimension $d+1$ is described by an effective spin model in d dimensions with short range interactions. In this spirit we use a strong coupling expansion for the $SU(N)$ YM theory in $3+1$ dimensions for obtaining effective theories formulated as $SU(N)$ spin models in three dimensions with a focus on $SU(3)$ YM.
We are thus lead to the following questions:

- How can effective models be constructed?
- What are the properties of such effective models?
- How can one relate YM (and perhaps QCD) to effective models in terms of obtaining couplings?

$SU(N)$ and characters of representations

We mainly deal with class functions on groups $SU(N)$. For this purpose we introduce representatives of a conjugacy class in the fundamental representation $(10\dots0)$ by

$$g = \mathrm{diag}(e^{i\phi_1}, \dots, e^{i\phi_{N-1}}, e^{-i(\phi_1+\dots+\phi_{N-1})}).$$

For the case of $SU(3)$ this leads to the reduced Haar measure on the maximal Abelian torus expressed in terms of ϕ_i by

$$d\mu_{\text{red}} = J^2 d\phi_1 d\phi_2, \quad J^2 = 15 - 6\chi_{11} + 3\chi_{30} + 3\chi_{03} - \chi_{22}.$$

Here we make use of the characters of representations of $SU(3)$, where e.g.

$$\mathcal{P} \equiv \chi_{10}(g) = \mathrm{tr}_{10}(g) = e^{i\phi_1} + e^{i\phi_2} + e^{-i(\phi_1+\phi_2)}.$$

By using the Young-tableaux technique we can express all characters in terms of the fundamental characters $\chi_{10\dots0}, \dots, \chi_{0\dots01}$. Specializing to $SU(3)$ these fundamental characters are $\mathcal{P}$ and $\mathcal{P}^*$, where the tableau according to χ_{pq} is given as follows:

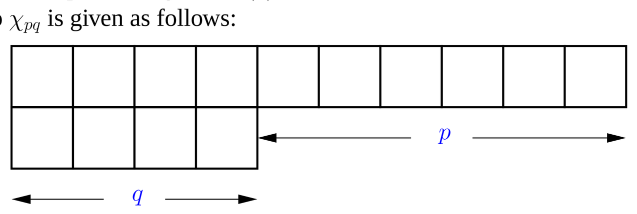

The effective models for YM

We start with the well-known Wilson action on the lattice

$$S_{\mathrm{W}} = \beta \sum_{\square} \left(1 - \frac{1}{N_C} \mathrm{Re}\ \mathrm{tr}\ U_\square\right), \quad \beta = \frac{6}{a^4 g^2}$$

and apply a strong coupling expansion (for small β). Since the resulting couplings are dimensionless there is no natural ordering scheme. Therefore we apply a truncation scheme combining following features:

- Ordering by powers of β. This is related to the dimension of corresponding representations.
- Ordering by distance of interacting Polyakov loops.

In compact form the strong coupling expansion is given by

$$S_{\text{eff}} = \sum_r \sum_{\mathcal{R}_1\dots\mathcal{R}_r} \sum_{\ell_1\dots\ell_r} c^{\ell_1\dots\ell_r}_{\mathcal{R}_1\dots\mathcal{R}_r}(\beta) \prod_{i=1}^{r} S_{\mathcal{R}_i,\ell_i}$$

with the basic building blocks

$$S_{\mathcal{R},\ell} \equiv \chi_{\mathcal{R}}(\mathcal{P}_{\boldsymbol{x}})\chi^*_{\mathcal{R}}(\mathcal{P}_{\boldsymbol{y}}) + \text{c.c.}, \quad \ell \equiv \langle \boldsymbol{xy} \rangle .$$

Here r counts the number of link operators contributing at each order. The coefficients $c^{\ell_1\dots\ell_r}_{\mathcal{R}_1\dots\mathcal{R}_r}$ are the couplings between the operators $S_{\mathcal{R}_i,\ell_i}$ sitting at NN links $\ell_i \equiv \langle \boldsymbol{x}_i, \boldsymbol{y}_i \rangle$ in representation $\mathcal{R}_i$. The effective action hence describes a network of link operators that are collected into (possibly disconnected) 'polymers' contributing with 'weight' $c^{\ell_1\dots\ell_r}_{\mathcal{R}_1\dots\mathcal{R}_r}$. Again, one expects the 'weights' or couplings to decrease as the dimensions of the involved representations and inter-link distances increase. In a strong coupling (small β) expansion truncated at $\mathcal{O}(\beta^{kN_{\mathrm{t}}})$ one has $r \le k$ and the additional restriction $|\mathcal{R}_1| + \dots + |\mathcal{R}_r| < k$ with $|\mathcal{R}| \equiv p+q$ for a given representation $\mathcal{R}$.

Effective models for $SU(3)$ YM

To lowest order $\mathcal{O}(\beta^{N_{\mathrm{t}}})$ one finds the universal effective action

$$S_{\text{eff}} = c_{10} \sum_{\langle \boldsymbol{xy} \rangle} S_{10,\langle \boldsymbol{xy} \rangle} \equiv \lambda_1 \sum_{\langle \boldsymbol{xy} \rangle} (\mathcal{P}_{\boldsymbol{x}}\mathcal{P}^*_{\boldsymbol{y}} + \mathcal{P}^*_{\boldsymbol{x}}\mathcal{P}_{\boldsymbol{y}}).$$

Our truncated model in order $\mathcal{O}(\beta^{2N_{\mathrm{t}}})$ and with nearest neighbour interactions reads as

$$S_{\text{eff}} = \lambda_1 \sum_{\langle \boldsymbol{xy} \rangle} (\chi_{10}(\mathcal{P}_{\boldsymbol{x}})\chi_{01}(\mathcal{P}_{\boldsymbol{y}}) + \text{c.c.}) + \lambda_2 \sum_{\langle \boldsymbol{xy} \rangle} (\chi_{20}(\mathcal{P}_{\boldsymbol{x}})\chi_{02}(\mathcal{P}_{\boldsymbol{y}}) + \text{c.c.})$$
$$+ \lambda_3 \sum_{\langle \boldsymbol{xy} \rangle} (\chi_{10}(\mathcal{P}_{\boldsymbol{x}})\chi_{01}(\mathcal{P}_{\boldsymbol{y}}) + \text{c.c.})^2.$$

Inverse Monte-Carlo – the basics

First we use the Wilson action to generate gauge configurations. These are reduced to Polyakov loop configurations from which we generate via IMC the couplings of a truncated effective action.

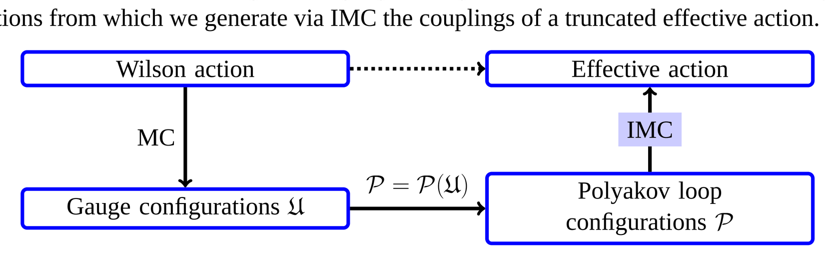

The Schwinger-Dyson (SD) based IMC procedure makes use of an ansatz for the effective action and some suitable operators which are used in SD equations for the determination of the corresponding effective actions (see [3, 4]). Generically the system of linear equations for the λ_i is overdetermined so that one has to use least-square methods for solving. A second way to determine the couplings of the effective theory is the demon method.

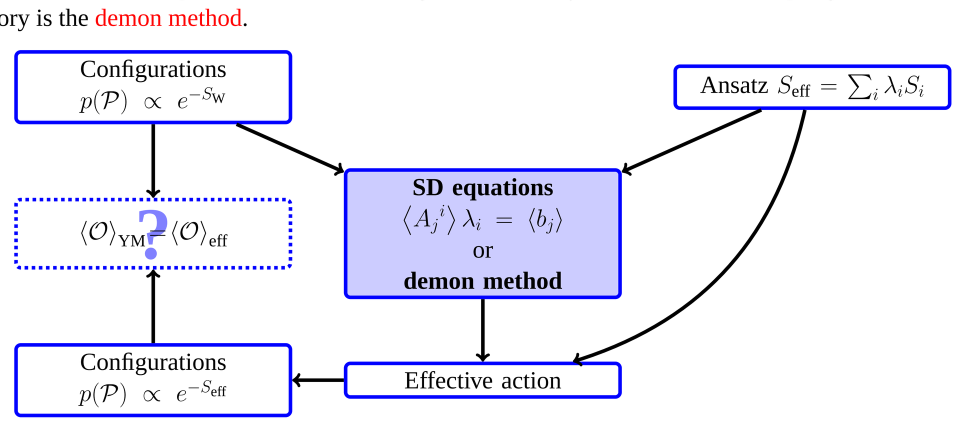

Finally the resulting effective action is used to compare expectation values with the microscopic YM theory.

Microcanonical demon method

Based on the large volume relation between microcanonical and canonical ensemble in statistical physics demon methods use additional degrees of freedom (called "demons") to simulate the effective theory together with the demons at a fixed total energy/action. This amounts to measure the coupling of the corresponding part of the effective action using the associated demon as a kind of "thermometer".
To simulate a microcanonical system with action $S[\mathcal{P}] = \sum_i \lambda_i S_i[\mathcal{P}]$ we transform the canonical measure to the microcanonical one,

$$\rho[\mathcal{P}, E_{\mathrm{D}}] \propto \exp\left(-\sum_i \lambda_i (S_i[\mathcal{P}] + E^i_{\mathrm{D}})\right) \quad \longrightarrow \quad \delta[S_i[\mathcal{P}] + E^i_{\mathrm{D}} - E^i_{\text{total}}].$$

For measuring the couplings we observe that each demons' energy E^i_{D} is distributed according to $\rho(E^i_{\mathrm{D}}) \propto \exp(-\lambda_i E^i_{\mathrm{D}})$ with λ_i depending on $\langle S_i \rangle$. Constraining the energies to some interval $E^i_{\mathrm{D}} \in [-E^i_0, E^i_0]$, $E^i_0 < \infty$ leads to an invertible relation $\langle E^i_{\mathrm{D}} \rangle = f_i(\lambda_i)$.
To obtain couplings via the demon method we perform the following steps:

1. Simulate the microscopic (full YM) system without additional demons using your preferred algorithm.
2. Take a well thermalized configuration and reduce the system to a Polyakov loop configuration as described in the IMC procedure.
3. Perform a microcanonical simulation of the reduced Polyakov loop system with coupled demons. As discussed below the thermalization procedure should be handled cautious.
4. Finally the mean energy of the demons is directly related to the couplings of the effective theory.

Tuning the microcanonical demon

- When using the microcanonical method we take one YM configuration and reduce it to a Polyakov loop configuration as a starting point for the microcanonical run. Therefore the method is highly sensitive to the chosen starting configuration.
  - In our simulations we can observe the effect of choosing start configurations with $S_i|_{\text{config}}$ in the vicinity of $\langle S_i \rangle_{\mathrm{YM}}$.
- Another parameter to be chosen is the energy range defined by E^i_0. When taking this range too small the demon has problems to thermalize due to a small acceptance rate in the update steps. For a much higher value of E^i_0 the demon is able to (and generically does) take much energy away from the effective system. This leads to effective configurations within the microcanonical ensemble which are almost independent of the starting configuration after the reduction step. Our way to circumvent these problems is the following:
  - Choose a large energy range $[-E^i_0, E^i_0]$ of the order $\mathcal{O}(|\langle S^i \rangle_{\mathrm{YM}}|)$.
  - Reduce the YM configuration to the effective configuration C_0.
  - For a few times (10 in our case) perform microcanonical simulations. The demons' start energies are given by the expectation value $\langle E^i_{\mathrm{D}} \rangle$ in the preceding run. The input configuration for the effective system is C_0 in every run.
  - The final run lasts for the same Monte-Carlo time as the preceding runs and is used to measure $\langle E^i_{\mathrm{D}} \rangle$ to obtain the effective couplings β_i.
- The contact between microscopic and microcanonical system is based only on one configuration. Further improvements should be possible by using a canonical demon method with more "thermal contact" to the microscopic system.

Canonical demon method

In order to use the full statistics of the microscopic system we apply the following algorithm:

1. Simulate the microscopic system according to $e^{-S_{\mathrm{W}}}$ until thermalization.
2. Perform the reduction of the microscopic system to the effective system.
3. Perform N_{micro} microcanonical updates of the joined system (effective+demon). These updates do not change the total energy $S^i + E^i_{\mathrm{D}}$.
4. Freeze the demon system and update the microscopic fields up to a new independent configuration. After that proceed again with step 2.

To deal with thermalization effects of the demons' energies we begin the measurement after N_{thermal} microscopic configurations.

Observables for $SU(3)$

We discuss the YM theory on a $N_{\mathrm{s}}^3 \times N_{\mathrm{t}}$ lattice. For measurements of the Polyakov loop we introduce the lattice-averaged Polyakov loop by

$$P \equiv \frac{1}{V} \sum_{\boldsymbol{x}} \mathcal{P}_{\boldsymbol{x}}, \quad V = N_{\mathrm{s}}^3.$$

Since in our analysis of the effective theories we deal with phases where the traced Polyakov loop points in the opposite direction of centre elements of $SU(3)$ we project the value of the traced Polyakov loop onto the nearest $\mathbb{Z}_3$-axis and define the rotated Polyakov loop by

$$P_{\text{rot}} = \begin{cases} \mathrm{Re}\, P & : P \in \mathcal{F} \\ -\frac{1}{2}\mathrm{Re}\, P + \frac{\sqrt{3}}{2}\mathrm{Im}\, P & : P \in \mathcal{F}' \\ -\frac{1}{2}\mathrm{Re}\, P - \frac{\sqrt{3}}{2}\mathrm{Im}\, P & : P \in \mathcal{F}'' \end{cases}.$$

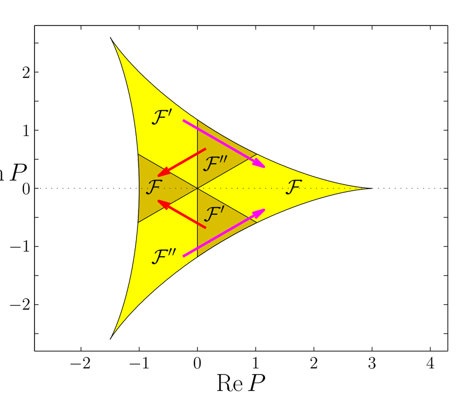

The confinement-deconfinement transition

We simulated the phase transition in $SU(3)$ YM on a $12^3 \times 2$ lattice using the standard Wilson action to obtain expectation values of the rotated Polyakov loop as an order parameter for confinement. Afterwards we used IMC with the SD equations as well as the (micro)canonical demon method for deriving couplings of the truncated effective theory.
The programming codes of the coupling computations were checked by simulating effective theories with fixed couplings and reproducing them consistently with the SD equations and the demon method.
All our simulations of this phase transition take place on the marked line on the upper border of the full YM phase diagram below. Here we can compare the results of the different methods: First we compute the couplings corresponding to one YM coupling β, and afterwards we use these couplings to simulate the corresponding effective theories with a Metropolis algorithm. The resulting expectation values of the rotated Polyakov loop are given as follows:

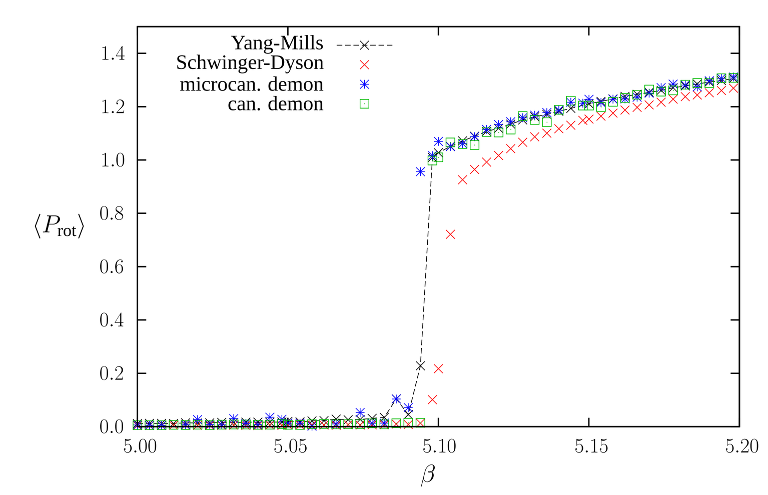

On this phase diagram we see that the SD equations fail to reproduce the correct critical point of the phase transition whereas the demon method reproduces $\langle P_{\text{rot}} \rangle$ near the phase transition and shows a better behaviour than the SD method in the vicinity of the critical coupling.

The effect of an adjoint particle

Due to a recent work by Myers and Ogilvie [6] the effect of an adjoint particle of mass M to the effective potential at one loop order is an additional potential term

$$\Delta V_{\text{eff}} = -\left[\frac{(2s+1)M^2T^2}{\pi^2} K_2(M/T)\chi_{11}(\mathcal{P})\right] = T\, h\, \chi_{11}(\mathcal{P}).$$

Here s is the spin of the particle and T corresponds to the temperature. Generically the parameter h is negative. Nevertheless topological excitations allow for a positive h and we therefore study a lattice action

$$S = \beta \sum_{\square} \left(1 - \frac{1}{N_C} \mathrm{Re}\ \mathrm{tr}\ U_\square\right) + H \sum_{\boldsymbol{x}} \chi_{11}(\mathcal{P}_{\boldsymbol{x}})$$

with the standard $SU(3)$ Wilson action and the adjoint term with an unconstrained parameter H.
On a $12^3 \times 2$ lattice we have simulated the system near the confinement-deconfinement phase transition varying β and H. In terms of the rotated Polyakov loop P_{rot} we obtain a phase diagram:

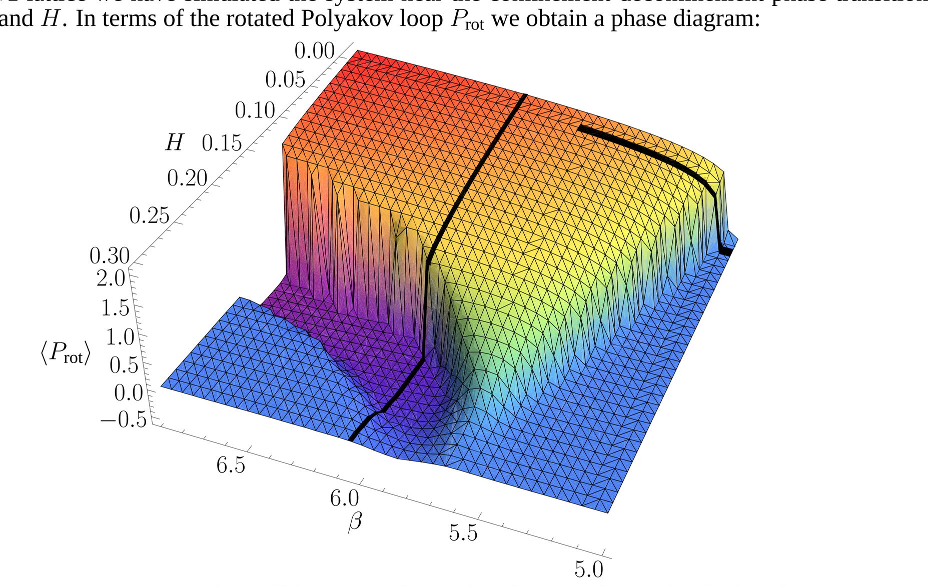

This diagram shows at $H = 0$ the well-known undirected and centre-directed Polyakov loop structures related to (de)confinement. In the lower half-plane an additional structure arises where the Polyakov loop points into "anti-centre" direction.
When evaluating the strong coupling expansion of the YM theory the additional potential term is already contained in the nearest neighbour expansion to $\mathcal{O}(\beta^{2N_{\mathrm{t}}})$. We therefore not only analyse the confinement-deconfinement transition, but also look for a sensible analysis of the new anti-centre phase in terms of a three coupling effective model.

The anti-centre phase

As marked by the vertical line in the full YM phase diagram above in the $\beta - H$-plane we used both methods to obtain the effective models for the anti-centre phase for $\beta = 6.05$, too. The resulting effective models are again used for simulations and the rotated Polyakov loops are compared:

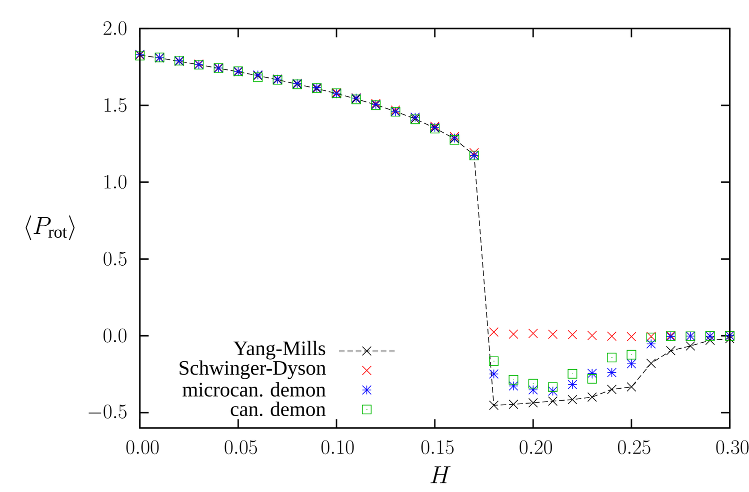

Whereas both methods have shown a quantitative difference in rendering the critical point near the (de)confinement transition the expectation values of P_{rot} indicate a big qualitative difference between the methods. While the SD method is able to produce a smooth behaviour with high accuracy deep in the deconfined phase it fails to reproduce the anti-centre phase completely. In contrast the demon methods are sensible to the full phase structure. To analyse the behaviour in the anti-centre phase we performed about 750 microcanonical runs at $\beta = 6.05$, $H = 0.2$ with different randomly chosen start configurations. The resulting couplings are plotted in the three coupling phase diagram of the effective theory:

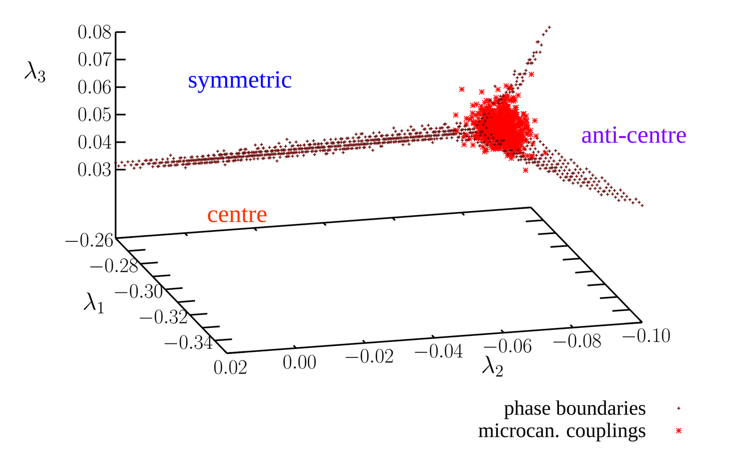

The phase diagram also shows a symmetric, centre directed and anti-centre directed phase as marked in the plot. Our results indicate that even far away from a phase transition in the microscopic theory the corresponding effective theory can be located in the vicinity of a phase transition.

Using thermalized configurations for the microcanonical demon

When using the microcanonical demon method we can choose the starting configuration randomly from the full YM ensemble. In contrast we are able to take configurations with $S_i|_{\text{config}}$ in the vicinity of $\langle S_i \rangle_{\mathrm{YM}}$ ("well thermalized"). On the three coupling model of $SU(3)$ YM we performed more than 100 microcanonical runs with these two different starting conditions resulting in a distribution in coupling space for $\beta = 6.05$, $H = 0$. The obtained couplings are shown in a projection to the λ_1-λ_2 plane:

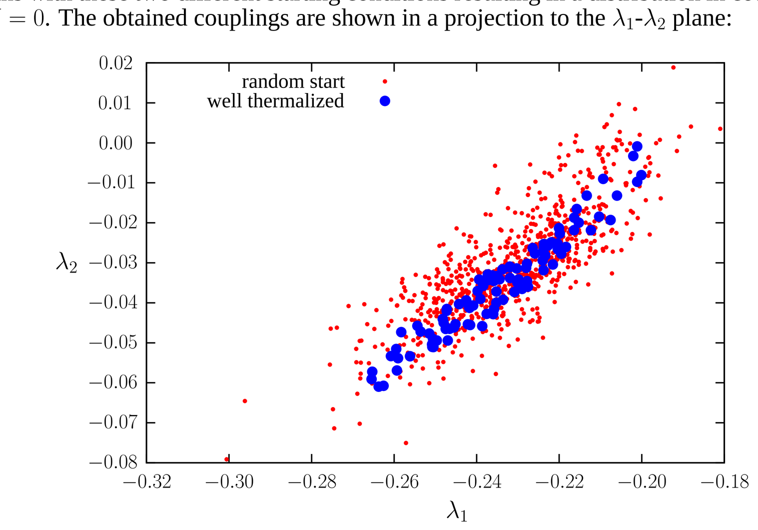

The extent of the derived coupling distribution shrinks for the well thermalized configurations compared to the randomly chosen configurations. As an additional feature the couplings of the well thermalized configurations correspond to almost the same rotated Polyakov loop whereas the couplings derived from the randomly chosen configurations show a much broader distribution of the corresponding rotated Polyakov loops.

Thermalization effects of the canonical demon

One open parameter of the canonical demon is the number of microcanonical sweeps per microscopic configuration N_{micro}. The distribution of the couplings can be analyzed in order to read off any thermalization effects. The microcanonical distribution serves as a reference.

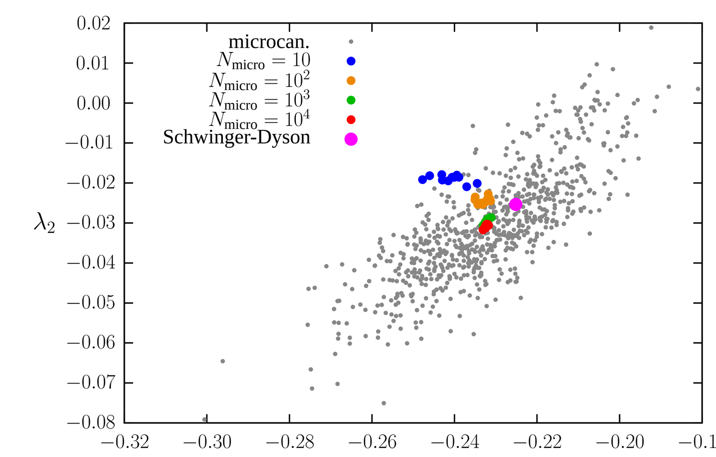

These results clearly show that the thermalization of the effective model has to be taken into account. With N_{micro} being small the effective system has not enough time to thermalize completely. The measured couplings refer to a non-equilibrium state of the effective model. Only in the large N_{micro} limit the couplings describe the thermal equilibrium of the effective model. According to [7] this behaviour is given by the fact that a configuration taken from a thermalized ensemble of the microscopic (YM) system is not necessarily a representative of an equilibrium state of the effective theory.
Furthermore we observe that the couplings obtained with the Schwinger-Dyson equations do not correspond to the ones computed with the canonical demon method.

Outlook to $SU(4)$ YM

For the finite temperature phase transition of the $SU(4)$ YM theory on a $6^3 \times 2$ lattice we can also apply the IMC method with the canonical demon method. Our effective model is a generalization of the effective model for $SU(3)$ YM:

$$S_{\text{eff}} = \lambda_1 \sum_{\langle \boldsymbol{xy} \rangle} (\chi_{100}(\mathcal{P}_{\boldsymbol{x}})\chi_{001}(\mathcal{P}_{\boldsymbol{y}}) + \text{c.c.}) + \lambda_2 \sum_{\langle \boldsymbol{xy} \rangle} (\chi_{010}(\mathcal{P}_{\boldsymbol{x}})\chi_{010}(\mathcal{P}_{\boldsymbol{y}}) + \text{c.c.})$$
$$+ \lambda_3 \sum_{\langle \boldsymbol{xy} \rangle} (\chi_{200}(\mathcal{P}_{\boldsymbol{x}})\chi_{002}(\mathcal{P}_{\boldsymbol{y}}) + \text{c.c.}) + \lambda_4 \sum_{\langle \boldsymbol{xy} \rangle} (\chi_{100}(\mathcal{P}_{\boldsymbol{x}})\chi_{001}(\mathcal{P}_{\boldsymbol{y}}) + \text{c.c.})^2$$

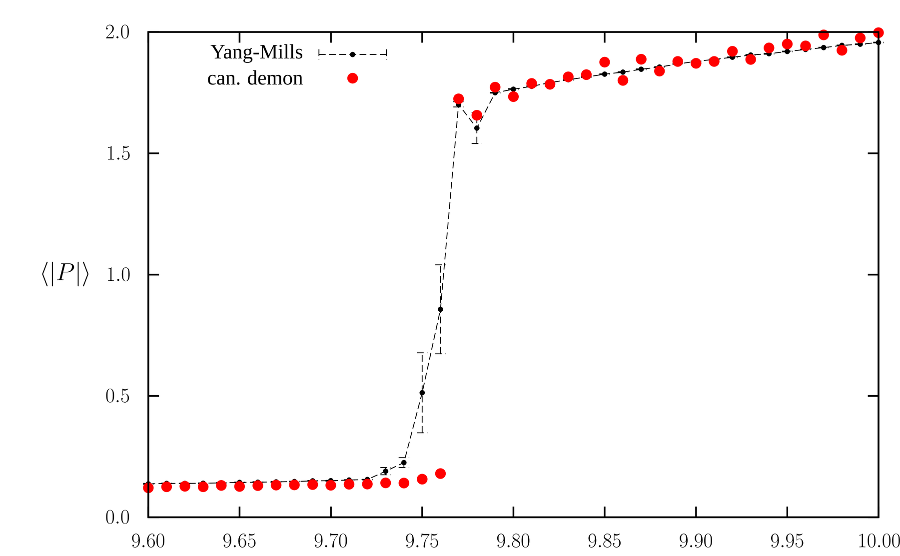

Even for $SU(4)$ the demon method is a robust way of obtaining couplings of effective Polyakov loop models describing the phase transition.

Conclusions

- The $SU(N)$ Yang-Mills theory is seen to be related to effective $SU(N)$ Polyakov loop models. To gain further insight into the details of this relation we studied and compared two ways of obtaining couplings for the effective theories.
- The application of the inverse Monte-Carlo method with SD equations to the $SU(3)$ YM case leads to stable results only far away from the phase transition. In the vicinity of the phase transition demon methods lead to a much better sampling of expectation values of the Polyakov loop.
- When we add an adjoint Polyakov loop potential to the Wilson action the phase diagram shows an anti-centre phase where the Polyakov loop points to the direction opposite to a centre element of $SU(3)$. This phase was tried to render by SD and demon methods. The SD method fails to recover the phase structure while demon methods are more favourable even in this case.
- The demon method can be generalised straightforward to the case of $SU(4)$ YM leading to robust results in the vicinity of the (de)confinement transition.
- Combining our experiences with both methods we see that SD equations are less efficient than demon methods on first order phase transitions although they have proven to be very useful for second order phase transitions in $SU(2)$ YM theories.
- When using demon methods much care has to be taken for the discussion of different thermalization effects. Firstly with microcanonical demons the way of choosing microscopic configurations influences the derived couplings. Secondly in the application of the canonical demon method thermalization effects (which can not be cured as discussed in [7]) must be taken into account.

References

[1] C. Wozar, T. Kaestner, A. Wipf, T. Heinzl and B. Pozsgay, "Phase structure of Z(3) Polyakov loop models," Phys. Rev. D **74** (2006) 114501 [arXiv:hep-lat/0605012].

[2] A. Wipf, T. Kaestner, C. Wozar and T. Heinzl, "Generalized Potts-models and their relevance for gauge theories," SIGMA **3** (2007) 006 [arXiv:hep-lat/0610043].

[3] S. Uhlmann, R. Meinel and A. Wipf, "Ward identities for invariant group integrals," J. Phys. A **40** (2007) 4367 [arXiv:hep-th/0611170].

[4] C. Wozar, T. Kaestner, A. Wipf and T. Heinzl, "Inverse Monte-Carlo determination of effective lattice models for SU(3) Yang-Mills theory at finite temperature," Phys. Rev. D **76**, 085004 (2007) [arXiv:0704.2570 [hep-lat]].

[5] T. Heinzl, T. Kaestner and A. Wipf, "Effective actions for the SU(2) confinement-deconfinement phase transition," Phys. Rev. D **72** (2005) 065005 [arXiv:hep-lat/0502013].

[6] J. C. Myers and M. C. Ogilvie, "New Phases of SU(3) and SU(4) at Finite Temperature," arXiv:0707.1869 [hep-lat].

[7] E. T. Tomboulis and A. Velytsky, "Renormalization group therapy," Phys. Rev. D **75**, 076002 (2007) [arXiv:hep-lat/0702015].